Materials Science in Semiconductor Processing 50 (2016) 31–35

Contents lists available at ScienceDirect

Materials Science in Semiconductor Processing

journal homepage: www.elsevier.com/locate/mssp

Transition of nanocrystalline $In(OH)_3$ as spherical Indium Oxide nanoparticles embedded platelets

S. Karthik Kannan [a], P. Thirnavukkarasu [a,*], R. Jayaprakash [b], J. Chandrasekaran [b], V. Mohanraj [b]

[a] Department of Electronics, Sri Ramakrishna Mission Vidyalaya College of Arts and Science, Coimbatore 641020, India
[b] Nanotechnology Laboratory, Department of Physics, Sri Ramakrishna Mission Vidyalaya College of Arts and Science, Coimbatore 641020, India

ARTICLE INFO

Article history:
Received 22 February 2016
Received in revised form
12 April 2016
Accepted 17 April 2016
Available online 27 April 2016

Keywords:
Indium oxide
Co-precipitation method
Crystal structure
X-ray diffraction and transmission electron microscopy

ABSTRACT

Indium oxide nanoparticles were synthesized by a co-precipitation method using the basic raw materials like Indium (III) Chloride and the precipitating reagent as Ammonium hydroxide. The formation of Indium oxide is highly dependent on temperature. The morphology, structural, particle size, optical and electrical properties of In_2O_3 nanoparticles were characterized by transmission electron microscopy (TEM), scanning electron microscopy (SEM), energy dispersive microscopy (EDS), X-ray diffraction (XRD), Fourier transform infrared radiation (FTIR), UV spectra, Photoluminescence spectroscopic (PL) and Electrical resistance measurements. The results exhibit a crystalline cubic structure in particles, spherical shape, size about 14 nm and optical band gap of 4.20 eV.

1. Introduction

Indium Oxide (In_2O_3) is an n-type semi conducting behavior with wide band gap around 3.6 eV at room temperature. Moreover it has high intrinsic electrons concentration with good mobility, and the possibility of quantum confinement effects in very small nanoparticles. In_2O_3 exhibits unique properties such as high electrical conductivity and optical transparency in the visible region [1]. Now a days In_2O_3 nanoparticles has attracted much attention of researchers mainly due to its tremendous applications in the Solar cell [2], field-emission display [3], lithium-ion battery [4], nanoscale biosensor [5], non-volatile Nano-floating gate memory [6], gas sensor [7], optoelectronics [8], photo catalysis [9], and field effect transistor [10]. Up to now, a wide variety of synthesis methods has been exploited such as sonochemical [11], Solution [12], template based method [13], chemical vapor deposition [14] and hydrothermal synthesis [15]. Among these methods the co-precipitation is considered for the preparation of Indium oxide nanoparticles because it is simple and cost effective. This method is also supported to get higher yield rate of nanopowder. The present work is focused as the conversion of good crystalline $In(OH)_3$ towards In_2O_3 nanoparticles. The factors supported for this transformation is discussed.

2. Experimental details

0.1 M aqueous solution of Indium (III) Chloride was prepared. Then pH of the solution was maintained at 8 using Ammonium hydroxide, $In(OH)_3$ precipitate formed was washed in de ionized water until the complete removal of chlorine ions. The precipitate was transferred into round bottom flask with 100 ml of de ionized water. The total solution was stirred for 5 h at 70 °C. During the stirring process the color of the solution becomes milky white. Again, the precipitate was filtered and dried around 120 °C followed by annealing at 220 °C and 330 °C for 3 h and resultant fine powder exhibits light yellow color respectively. The crystalline nature of the above mentioned samples was analyzed form X-Ray Diffraction (XRD) using X' pert PRO PAN'alytical. The Fourier Transformation Infrared (FTIR) analysis was carried with a Perkin Elmer Spectrum RXI spectrometer for the wavelength ranging from 400 nm to 4000 nm. The morphology of the prepared sample was studied from Scanning Electron Microscopy (SEM) image which were recorded from Hitachi S3200 and Transmission Electron Microscopy (TEM) was recorded on a Philips mod CM200. The Indium oxide sample under investigation by SEM can be mounted on SEM stub by using conductive carbon tape. This loaded sample was subjected for scanning and recorded the morphology. A small quantity of annealed sample at 330 °C of Indium oxide is mixed in ethanol and dispersed as a very thin layer on the carbon film coated TEM grids and which is dried thoroughly. Then this sample is subjected to view TEM image. Optical absorption spectrum was

* Corresponding author.
E-mail addresses: skarthikkannan@yahoo.co.in, kkarathana@yahoo.in (S.K. Kannan).

http://dx.doi.org/10.1016/j.mssp.2016.04.010
1369-8001/

recorded on a Cary 5E UV–vis NIR recording spectra-photometer with the wavelength range of 200–300 nm at room temperature and The Photoluminescence spectra of the sample were collected from a JY Fluorolog-FL3-11 spectroflurometer. DC electrical resistance measurements are analyzed with the help of a Keithley electrometer 6517B.

3. Results and discussion

3.1. X-ray diffraction analysis

Fig. 1 shows the XRD patterns of the as-prepared sample and sintered samples at 220 °C and 330 °C. The XRD pattern of the as prepared sample Fig. 1(a) has exhibited the following hkl values (200), (220), (013), (222), (400), (420), (422), (440) and (620) which matches well with standard JCPDS card #85-1338 of In $(OH)_3$ crystal and structure of the crystal is found to be cubic. The average crystallite size (D) was calculated from Debye Scherrer's formula [16]:

$$D = \frac{K\lambda}{\beta\cos\theta}$$

where D is the mean crystalline size, K is a grain shape dependent constant (0.9), λ is the wavelength of the incident beam, θ is a Bragg reflection angle and β is the full with half maximum (FWHM) of the maximum intense peak in the X-ray diffraction pattern. The particle size is found as 24 nm. The lattice constant is calculated for $In(OH)_3$ as 7.93776 (Å) is determined by the following relation:

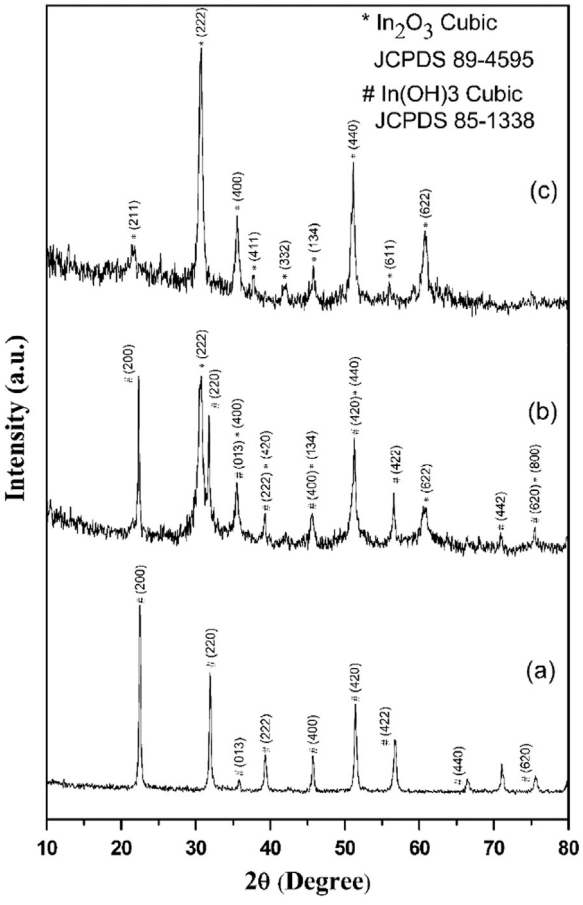

Fig. 1. XRD patterns of indium oxide nanoparticles (a) as-prepared, (b) annealed at 220 °C (c) annealed at 330 °C.

$$\frac{1}{d^2} = \frac{(h^2 + k^2 + l^2)}{a^2}$$

where d is the inter planar distance of the diffraction planes and (hkl) are the miller indices. Also crystallinity level of $In(OH)_3$ is indicated that the obtained In $(OH)_3$ are in phase in which sufficient reaction has taken place and employed temperature is also adequate. The temperature is given for the reaction is significant factor to the attainment of $In(OH)_3$ phase. The prominent peak of [200] shows the preferred growth of $In(OH)_3$ crystallites [17]. Fig. 1 (b) and (c) show the XRD patterns of the samples for the sintering conditions at 220 °C and 330 °C. The peaks in the XRD patterns in Fig. 1(b) revealed that mixed crystallites phases of $In(OH)_3$ and In_2O_3 and their respective hkl values are (200), (220), (013), (222), (400), (420), (422), (442), (620) (JCPDS card #85-1338) and (222), (400), (420), (134), (440), (622), (800) (JCPDS card #89-4595) respectively. When the $In(OH)_3$ sample is heated for 220 °C (Fig. 1 (b)), there is a phase transformation is started and new peaks are emerging along with $In(OH)_3$ peaks due to the process of heating and the peak corresponding (440) plane is absent when compared with as-prepared samples. The intensity of the peak are increased slightly and few prominent additional peaks are identified in preferred orientations such as (222), (622). The intensity of the peak corresponding to (222) plane has enhanced enormously. Thus it confirms that the growth of crystallinity in this preferred orientation is more [18]. Thus the heating process induced that the specific planes of $In(OH)_3$ have involved to the phase transformation from $In(OH)_3$ to In_2O_3. The average lattice constant is calculated as 8.051 (Å) for $In(OH)_3$ which is almost nearer to the lattice constant value obtained for as prepared sample. Also the lattice constant value measured for In_2O_3 phase is 10.129 (Å) for the same sample. The crystalline size is calculated as 22 nm for In $(OH)_3$ and 14 nm for In_2O_3 nanoparticles. When the temperature is further raised to 330 °C Fig. 1(c). The $In(OH)_3$ peaks are disappeared and becomes cubic structured In_2O_3 phase. This sample consist of only In_2O_3 phase rather than the presence of $In(OH)_3$. The identified characteristic peaks belong to hkl values of (211), (222), (400), (411), (332), (134), (440), (611) and (622) (JCPDS card #89-4595) [19]. The lattice constant a is calculated as 10.101 (Å) [20] and the obtained value is almost nearer to the value of In $(OH)_3$ in the mixed phase. The lattice parameters calculated are less than the bulk material value of 10.118 (Å) [21]. This may be due to the phenomenon of lattice concentration developed in the powder. The particle size is predicted for this sample as 14 nm. It was confirmed that heating process transforms Indium hydroxide into Indium oxide. The structure and preferred orientation is depending upon the annealing temperature. The crystallinity is formed due to the removal of hydroxyl group in the material and there is an occurrence of the structural change which promotes the good crystallinity.

3.2. Fourier transform infrared

Infrared analysis of the sample was performed on a FTIR spectrometer in transmission mode ranging from 400 to 4000 cm^{-1}. Fig. 2(a) and (b) shows the FTIR spectra of as prepared and sintered samples at 220 °C. Fig. 2(c) shows the IR spectra of the sintered powder at 330 °C. The broad band in the range 3500–2750 cm^{-1} is due to the OH stretching vibrations [22]. In these spectra a strong absorption broad band at around 3423 cm^{-1} characteristics of OH stretching is observed and week band around 1157 cm^{-1} [22]. The In-O band emerges at wave number of 1596 cm^{-1}. Other absorption bands between ~1355 and ~ 491 $cm^{-1}$are assigned to In-OH groups [23] and band deformation of water due to the thermal treatment. It is observed that the intensity of the respective peaks of 1155 cm^{-1} and 777 cm^{-1}